JSER

Journal of Solar Energy Research (JSER)

Journal homepage: www.jser.ut.ac.ir

# Design of Parallel Boost Converters for Renewable Energy Applications

Arunyuvaraj Kuppusamy[a*], Venkatesh Perumal Mahalingam[b,]

[a,b] *Department of Electrical and Electronics Engineering, Vignan's Foundation for Science, Technology & Research, , P.O. Box: 522213 , Guntur, India.*

**ARTICLE INFO**

**Article Type:**

**Research Article**

**Received:29.11.2023**
**Accepted:27.09.2024**

**Keywords**:
Boost converter,
Sliding variable,
CPOT controller,
P&O formula,
Total harmonic distortion

**A B S T R A C T**

To achieve effective electrical power conversion from both the photovoltaic (PV) system and the wind system, parallel-connected boost converters (PBC) are employed in this paper. A perturb and observe (P&O) formula-based concentrated power opinion tracing (CPOT) controller operates the PV and wind-operated permanent magnet synchronous generator, providing the input supply to the proposed converter. With the help of the PBC, the direct current (DC) voltage is increased and converted into a single-phase, 230Vrms, 50Hz alternating current (AC) voltage in a single-stage operation. For this DC power to AC power conversion, the system attempts to synchronize two different power sources. The sliding variable configuration control (SVCC) method is used to control the proposed PBC to obtain a constant AC output voltage from variable DC input voltage sources. The recommended control method has been applied to maintain the output voltage constant through changing load conditions. The implemented technique increases the performance of the power transition system while reducing total harmonic distortion (THD). The entire system is structured using the MATLAB/Simulink environment, which is utilized to validate the results.

## 1. Introduction

In recent decades, the energy production sector has adversely impacted public health primarily due to air pollution. To address these challenges, there is increasing recognition of the potential benefits of expanding the use of renewable energy resources (RER). Arash Mohammadi Sheikhlari and Mohammad Sarvi [1] emphasized the urgent need to boost clean energy generation by harnessing

*Corresponding Author Email:kayeee91@gmail.com

**Cite this article:** Kuppusamy, A., & Mahalingam, V. (2024). Design of Parallel Boost Converters for Renewable Energy Applications. Journal of Solar Energy Research, 9(3), 1954-1965. doi: 10.22059/jser.2024.368785.1359

DOI: 10.22059/JSER.2024.368785.1359

available renewable energy resources, responding to global concerns about environmental change and fossil fuel depletion.

Soundarya et al. [2] noted a shift towards alternative energy sources driven by reduced reliance on traditional sources and heightened pollution concerns. This transition was facilitated by advancements in various RER technologies, such as photovoltaic and wind, offering cost-effectiveness, reduced pollution, environmental friendliness, and improved energy security. While wind and solar energies have been extensively studied in developed nations, research in developing nations remains limited despite potentially significant health benefits varying with local conditions. Current research highlights the substantial health benefits of RER adoption, essential in energy project cost-benefit analyses, as noted by Silva et al. [3]. However, no single RER source guarantees continuous power availability.

To meet energy demands and enhance security, hybridizing at least two renewable sources is imperative, as stated by Kong et al. [4]. Thus, optimizing the interface conversion efficiency of these hybrid systems plays a crucial role. While extensive literature exists on hybrid power generation systems, not all configurations are universally applicable, and specific limitations must be considered. Integrating diverse RER sources requires careful assessment of factors like efficiency improvement, cost-effectiveness, and resource availability to design effective power conversion systems.

Alatai et al. [5] and Parimalasundar Ezhilvannan et al. [6] emphasized the rapid development of modern energy applications, including smart grids, electric vehicles, and photovoltaic systems, highlighting the critical role of DC-DC converters in meeting industrial demands. Designing a single converter capable of effectively powering diverse modern energy systems and interacting seamlessly with energy storage options remains a significant challenge. Converter enhancements have successfully reduced switching losses and improved energy conversion efficiency. Qianwen Xu et al. [7] suggested bidirectional DC-DC converters with galvanic isolation as optimal for hybrid energy configurations due to fewer semiconductor switches, reduced harmonic distortion, and lower voltage stress on semiconductor components. Comprehensive evaluations of various bidirectional converter types, including multilevel and conventional inverters, have driven bidirectional DC-DC converter advancements.

Elkin Edilberto Henao-Bravo et al. [8] pioneered stand-alone power conversion systems utilizing bidirectional DC-DC technology and RER. These systems utilized an energy storage system (ESS) comprising a bidirectional DC-DC converter and a DC bus, coupled with a charger/discharger power converter. Alhuwaishel and Prasad Enjeti [9] developed an ESS implementation without electrolytic capacitors using circuit analysis techniques. Their charger/discharger DC-DC converter employed a single sliding-mode controller (SMC) to maintain constant DC bus voltage under varying operating conditions, as implemented by Karthikeyan et al. [10]. Han Li et al. [11] acknowledged the pulse-width modulation-based SMC controller's effectiveness in mitigating parameter drift and delay issues, maintaining system stability even with the converter's inherent nonlinearity. The controller dynamically adjusted SMC parameters based on variables like ESS current and DC voltage error, ensuring optimal system performance.

Haifeng et al. [12] implemented a solar-biomass hybrid power generation system that integrates solar thermal energy collection with a biomass steam boiler and steam turbine power production. Challenges included system constraints based on biogas and intermittent availability of cow dung for fuel, requiring careful management of plant scalability and energy conversion efficiency. Pires et al. [13] discussed efforts to develop universal converters using external connectors for seamless operation within both DC and AC grids, aimed at simplifying the integration of energy storage systems and RER. This design reduced redundant power switches and passive components, enabling interaction with DC/AC grids and loads. While initial universal converter designs focused on AC single-phase power conversion systems, modular extensions and pulse-width modulation approaches expanded these capabilities.

Ligang Wu et al. [14] explored the adaptability of sliding-mode control in various power converter applications, highlighting its robustness in handling parameter uncertainty and external disturbances. However, variable switching frequencies in power converters could lead to increased losses and challenges in filter design, further complicated by the complexity of modern power systems driven by RER integration. Future developments in sliding-mode control may be necessary to effectively manage large-scale and complex converters.

Namrata Bist and Anirbid Sircar [15] discussed hybrid power systems combining geothermal and solar energy sources, noting geothermal power's ability to produce electricity without greenhouse gases. Remote area power supply systems often use hybrid power systems combining solar PV and wind energy technologies, with dual-leg DC-AC converters supporting wind and solar integration. Abdelkarim Masmoudi et al. [16] and Handrata Roy Josiaa [17] discussed solar-based converters for power conversion, output voltage control, and power conditioning. However, managing solar energy efficiency and battery storage costs remains critical in multisource power conversion systems.

Billel Talbi et al. [18] proposed a model predictive voltage control strategy to enhance single-phase inverter output voltage control in stand-alone renewable energy systems. Noor Syafawati Ahmad et al. [19] introduced single-phase grid-connected inverters with simplified sinusoidal pulse-width modulation (SPWM) control, enhancing power flow control using a low-cost microcontroller unit. Elnozahy et al. [20] explored voltage control and current regulation methods using sliding-mode controllers on the inverter side, adapting to varying solar radiation and wind speed conditions.

Vijayakumar Arun et al. [21] proposed an asymmetrical single-phase nine-level inverter generating a staircase-like voltage pattern using level-shifted pulse-width modulation, suitable for asymmetric DC voltage sources like those in electric vehicles and AC mini-grids powered by RER. Leonardo Callegaro et al. [22] developed a grid-connected photovoltaic inverter with a feedback linearization-based controller for stable PV input voltage regulation.

The analysis addressed efficiency concerns and practical challenges associated with current multilevel inverter topologies, including cost, complexity, and performance across varied conditions. The evaluation focused on optimal methods for integrating and sizing solar and geothermal energy sources to enhance system reliability and efficiency, while also assessing environmental impacts and economic viability compared to standalone systems. The study examined computational demands and implementation challenges of model predictive control for single-phase inverters, analysing transient response and control effectiveness under changing loads and grid conditions.

Trade-offs in inverter performance metrics such as grid synchronization, efficiency, and harmonic distortion were assessed, while advanced modulation strategies for improved grid-connected operation were developed. The evaluation covered optimization algorithm efficiency, convergence, and robustness, along with intelligent control techniques for optimizing photovoltaic output power and regulating DC-bus voltage. Practical challenges in implementing fuzzy integral sliding-mode control were studied, including hardware requirements for solar systems, control system resilience, and performance under diverse load profiles and weather conditions.

Sreenivasulu Reddy and Varaprasad Janamala [23] explored integrating RER into electrical distribution systems with the goals of minimizing power losses, reducing greenhouse gas emissions, and improving voltage stability. Their approach involved using a meta-heuristic pathfinder algorithm to determine the optimal placements and capacities for photovoltaic and wind energy systems, along with ESS and capacitor banks, in both grid-connected and islanded modes. Nasim Hashemian and Alireza Noorpoor [24] studied a multi-generation system that uses biomass and solar energy to produce electricity, heating, cooling, hydrogen, and potable water. The proposed system consists of several components, such as a steam Rankine cycle, a double-effect absorption chiller, a proton exchange membrane electrolyser, multi-effect desalination, and a parabolic trough solar collector.

From the literature, it became evident that several research gaps existed in power conversion systems for renewable energy sources. Existing systems often faced inefficiencies and reliability issues due to their lack of dynamic adaptability and real-time responsiveness to changing load conditions and input voltages. Many of these systems employed fixed-parameter control techniques, which lacked real-time tuning. This limitation resulted in slower reaction times, greater overshoot, and more steady-state errors. Additionally, conventional systems were less resilient to component variations and external disturbances and typically exhibited higher THD.

To address these gaps, there was a clear need for more sophisticated control systems capable of dynamically optimizing performance, akin to the sliding variable configuration control. Such advancements were essential to enhance efficiency, reliability, and overall power quality in renewable energy applications. The novelty of the sliding variable configuration control for parallel-connected boost converters was primarily attributed to several key advancements. It excelled in enhancing voltage boosting during single-stage operation, achieving a pure output voltage waveform without the need for additional filtering.

This approach maximized the utilization of input RER and offered dynamic flexibility by responding in real-time to varying load conditions and input voltages. Unlike conventional fixed-parameter control methods, the sliding variable approach enabled instantaneous parameter adjustments, leading to reduced overshoot, minimized steady-state errors, and significantly improved response times. As a result, this proposed control strategy enhanced voltage regulation, strengthened resilience against component variations and external disturbances, and increased efficiency by lowering THD in energy conversion systems. Its relative ease of implementation compared to advanced control techniques facilitated real-time applications with limited computational resources, enabling straightforward hardware realization and parameter tuning.

## 2. Parallel Connected Boost Converters

The proposed system integrated parallel-connected boost converters for combining solar PV and wind turbine power, as depicted in Figure 1. This configuration included a CPOT mechanism based on the P&O algorithm.

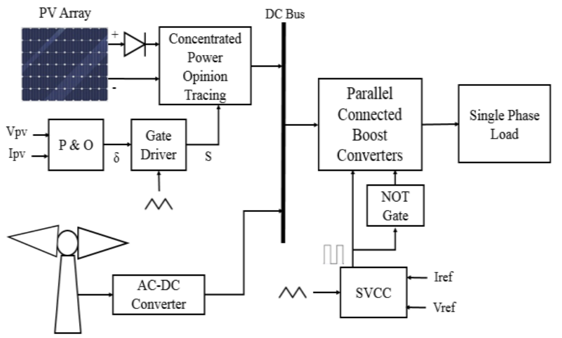


Figure 1. Detailed structure of proposed solar PV and wind system powered PBC

According to Ahmed Darwish et al. [25], CPOT improved PV panel performance by eliminating oscillating even-order harmonic components from the inverter's input, thereby optimizing power extraction. The P&O algorithm ensured a stable DC output despite fluctuations in the photovoltaic module's DC output, as highlighted by Haq et al. [26], Ibrahim [27], and Chigane & Ouassaid [28]. This algorithm operated by adjusting the PV system's operating point, either by varying voltage or current, and then observing the resulting change in power output. Continuously fine-tuning these conditions to maximize power output allowed the algorithm to effectively track the maximum power point. Its simplicity, low computational demands, and real-time effectiveness made it a preferred choice in PV systems, supported by studies such as those by Min Keng Tan et al. [29], Mousa et al. [30], and Trinh et al. [31].

The P&O algorithm and CPOT controller were pivotal in renewable energy systems, designed to optimize energy extraction, improve energy conversion efficiency, and adapt to environmental variables such as fluctuations in sunlight or wind speed, thereby enhancing overall system performance. In this integrated system, the output from the PV system was connected to a common bus, while the AC voltage produced by the wind turbine was rectified to DC before feeding into the same DC bus. This common bus voltage served as the input to the PBC. The proposed system performed dual functions: firstly, it boosted the DC voltage, and secondly, it converted DC power into single-phase AC power in a single-stage operation at the fundamental utility frequency. The PBC was controlled using the SVCC technique, ensuring that the output voltage of the converter remained constant, thereby supplying stable power to single-phase AC loads.

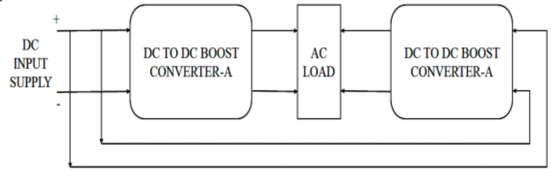


Figure 2. Block diagram of proposed PBC

Figure 2 depicted the proposed PBC block diagram, featuring two independent bidirectional DC-DC converters, labelled as converter-A and converter-B. These converters operated with a phase shift angle difference of 180 electrical degrees from each other. Each DC-DC boost converter generated a DC-biased sinusoidal voltage output, with each converter providing the maximum voltage differential across the load. The reference nodes of both converters were connected in common, while the positive terminals of each converter were connected to the load.

The PBC utilized SVCC to govern both converter-A and converter-B, ensuring robust, fast, and precise regulation of the output voltage. This configuration guaranteed reliable performance under varying operational conditions and environmental factors. The single-stage operation of the PBC, coupled with minimal power switches, maintained an uninterrupted sine wave output voltage without requiring additional filters, offering efficiency and simplicity in power conversion.

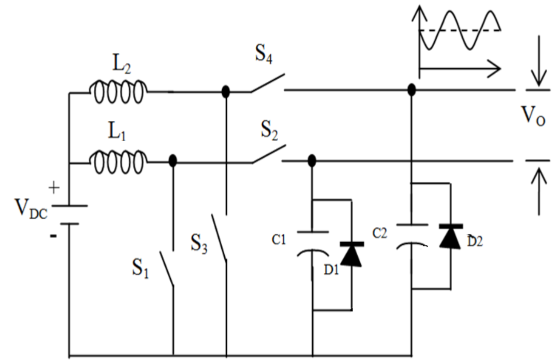


Figure 3. Circuit description of proposed PBC

Figure 3 illustrates the circuit configuration of the proposed PBC. It incorporated four primary switches—$S_1$, $S_2$, $S_3$, and $S_4$ along with two inductors ($L_1$ and $L_2$), two capacitors ($C_1$ and $C_2$), and two diodes ($D_1$ and $D_2$). Converter-A comprised $S_1$, $S_2$, $L_1$, $C_1$, and $D_1$, while converter-B includes $S_3$, $S_4$, $L_2$, $C_2$, and $D_2$. The PBC operated in two distinct modes: Mode 1 and Mode 2. In Mode 1, $S_2$ was activated, allowing current to flow through $L_1$, causing an increase in inductor current, while capacitor $C_1$ supplied power to the load. Consequently, the voltage across $C_1$ ($V_{bc1}$) decreased, while $S_1$ remained open. During Mode 2, $S_1$ closed while $S_2$ opened. This action transferred the source voltage $V_{DC}$ and the current from $L_1$ to the load, while also storing partial energy in capacitor $C_1$. These operational modes ensured efficient energy transfer and voltage regulation, essential for stable performance across varying load conditions in renewable energy applications.

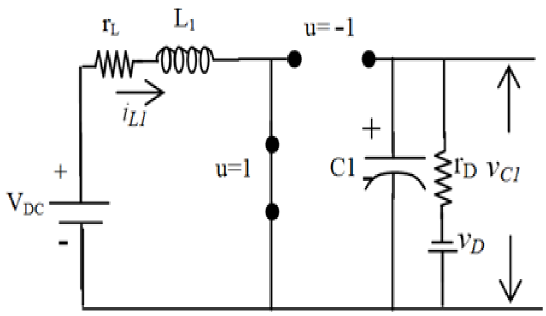


Figure 4. State modelling equivalent circuit of PBC

The state modelling equivalent circuit of the proposed PBC, depicted in Figure 4, was crucial for accurately representing the converter's dynamic behaviour and facilitating comprehensive analysis and control design. By formulating differential equations that captured internal states such as voltages, currents, and switching states, valuable insights into both transient and steady-state performance were gained. This modelling framework enabled the development and refinement of control strategies aimed at achieving specific performance objectives, such as voltage regulation and power flow management.

Furthermore, state modelling allowed for the simulation of the converter's response under varying operating conditions, enabling assessments of reliability, efficiency, and overall effectiveness. Ultimately, state modelling played a pivotal role in ensuring the efficient operation of PBCs serving as inverters across a range of applications, including renewable energy systems and electric vehicle powertrains. The conduction modes of boost converter-A and boost converter-B are defined by equations (1) [10] and (2) [10], where voltage control is achieved by regulating the duty ratio of the converter output.

$$\frac{V_{bc1}}{V_{dc}} = \frac{1}{1 - D_P} \tag{1}$$

$$\frac{V_{bc2}}{V_{dc}} = \frac{1}{D_P} \tag{2}$$

$D_P$ is the duty cycle, $V_{bc1}$ and $V_{bc2}$ are the voltages across the capacitors of converter-A and converter-B, respectively, and $V_{DC}$ is the input voltage to the PBC. Since the two parallel-connected converters are 180° out of phase, the output voltage equation is given by equation (3) [10].

$$V_o = V_{bc1} - V_{bc2} = \frac{V_{dc}}{1 - D_P} - \frac{V_{dc}}{D_P}$$

$$\frac{V_o}{V_{dc}} = \frac{2D_P - 1}{(1 - D_P)D_P} \tag{3}$$

## 3. Control Approach of a Parallel Connected Boost Converters

When Kirchhoff's voltage and current laws are applied to the equivalent circuit of parallel-connected DC to DC boost converters, as shown in equations (4) [8] and (5) [8], the state variables of converter-A are obtained as $i_{bc1}$ and $V_{bc1}$, which are represented in equations (6) [8] and (7) [8], respectively.

$$\frac{di_a}{dt} = \frac{v_{dc}}{L_1} - i\frac{r_L}{L_1} \quad (4)$$

$$\frac{dv_{bc1}}{dt} = \frac{dv_{bc2}}{r_{DC1}} - i\frac{r_L}{L_1} \quad (5)$$

$$\frac{v_{dc}}{L_1} - \frac{v_{bc1}}{L_1} - i\frac{r_L}{L_1} = \frac{di_{bc1}}{dt} \quad (6)$$

$$\frac{dv_{bc1}}{dt} = \frac{i}{c_1} - \frac{v_{bc1}}{r_{DC1}} + \frac{v_{bc2}}{r_{DC1}} \quad (7)$$

$$\begin{bmatrix} \bar{x} \\ \bar{\bar{x}} \end{bmatrix} = \begin{bmatrix} \frac{-r_L}{L_1} & \frac{-1}{L_1} \\ \frac{1}{C_1} & \frac{-1}{C_1 r_D} \end{bmatrix} \begin{bmatrix} i_{bc1} \\ v_{bc1} \end{bmatrix} + \begin{bmatrix} \frac{v_{bc1}}{L_1} \\ \frac{-i_{bc1}}{C_1} \end{bmatrix} u + \begin{bmatrix} \frac{v_{dc}}{L_1} \\ \frac{v_{bc2}}{C_1 r_D} \end{bmatrix} \quad (8)$$

Where $\bar{x}$ and $\bar{\bar{x}}$ are the vectors of the state variables ($i_{L1}$, $V_{c1}$). By considering the inductor resistance, the state-space model of the proposed system has been derived and is presented in equation (8) [14]. It is simplified and shown in equation (9) [14], where U represents the status of the switches.

$$\bar{X} = Ax + BU + C \quad (9)$$

$$U(i_{bc1}, v_{bc1}) = K_1 e_1 + K_2 e_2 = 0 \quad (10)$$

$$e_1 = i_{bc1} - i_{1ref} \quad (11)$$

$$e_2 = v_{bc1} - v_{1ref} \quad (12)$$

Equations (11) [14] and (12) [14] are substituted in (10) [14],

$$U = K_1(i_{bc1} - i_{1ref}) + K_2(v_{bc1} - v_{1ref}) \quad (13)$$

The status of the switches is determined by equation (13) [14]. When U is equal to 1, switch $S_1$ is ON and switch $S_2$ is OFF, as shown above. Conversely, when the value of U is equal to 0, switch $S_1$ is OFF and switch $S_2$ is ON. The sliding variable control equation in the state-space is formulated as a nonlinear combination of the state variable errors $\varepsilon_1$ and $\varepsilon_2$. These errors result in an excellent dynamic response in the output voltage.

The responses of the circuit parameters are characterized by coefficients $K_1$ and $K_2$, which are typically determined through a trial-and-error method. These coefficients are chosen to ensure a satisfactory response under sliding operating conditions while maintaining stability. In the context of controlling the output of the single-stage PBC, a sliding variable configuration control approach is recommended, as illustrated in Figure 5. This control approach involves dynamically adjusting the coefficients $K_1$ and $K_2$ to regulate the converter's output voltage effectively.

Sliding variable configuration control is particularly suited for applications where precise and robust control of the output voltage is critical, such as in renewable energy systems and electric vehicle powertrains. By continuously adjusting these coefficients, the control system can adapt to varying load conditions and input voltage fluctuations, ensuring stable and efficient operation of the PBC across different operating scenarios.

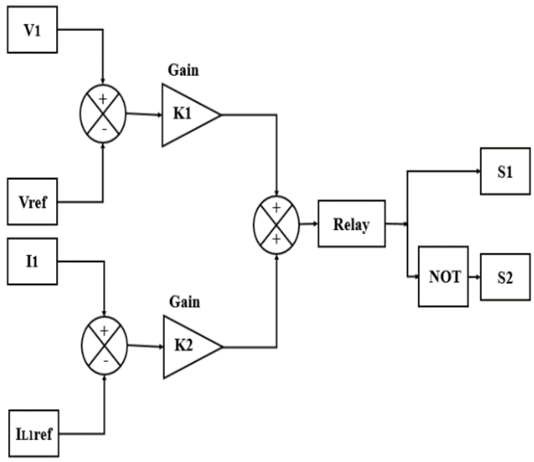


Figure 5. Proposed sliding variable configuration control strategy

The hysteresis current controller employed in the proposed converter system integrates the sum of error signals from state variables, along with specified gains, as discussed by Khamharnphol et al. [32]. This controller operates by defining lower and upper bands based on the ripple of these error signals, creating a continuous pulse signal with varying widths. The boundaries of these bands are adjusted to ensure stable operation within a frequency range up to 400 kHz, effectively managing load changes and maintaining closed-loop control stability.

The correct adjustment of the duty cycle for converter-A and the appropriate selection of gain values $K_1$ and $K_2$ are crucial. These adjustments enable precise control of the capacitor ($V_{bc1}$) and inductor current ($i_{L1}$) of converter-A. The pulse signals generated with varying widths control the power switches for converter-A. The same control method is applied to converter-B, but with a 180-degree electrical phase shift, ensuring efficient operation and management of the entire PBC. This approach ensures adaptive switching frequency control, optimizing performance across dynamic operational conditions encountered in practical applications.

## 4. Simulation Model

The design parameters of the proposed PBC power conversion system are shown in Table 1. By designing the proper inductor value, capacitor value, and switching frequency, the performance of the converter has been improved.

Table 1. Simulink parameters of the proposed parallel connected boost converters [33]

| S. No. | Parameter Name | Value |
|---|---|---|
| 1 | Converter input DC Voltage ($V_{DC}$) | 105V |
| 2 | PBC Output Voltage ($V_O$) | $230V_{rms}$ |
| 3 | Inductor $L_1$ | 760µH |
| 4 | Inductor $L_2$ | 760µH |
| 5 | Capacitor $C_1$ | 22µF |
| 6 | Capacitor $C_2$ | 22µF |
| 7 | Switching Frequency (Fs) | 400 KHz |
| 8 | Output Frequency | 50 Hz |

The strategy and modelling of the PBC for solar PV and wind power conversion systems have been implemented using the MATLAB/Simulink environment, as depicted in Figure 6. In this setup, the output DC voltage from the PV system is directed to the DC bus through a diode, ensuring that energy flow from the PBC to the PV system is prevented. By simulating the interactions between the PV system, wind turbine, and the PBC, engineers can evaluate performance metrics such as efficiency, voltage regulation, and power flow dynamics. Such simulations are essential for optimizing control strategies, validating system designs, and assessing overall system reliability under various operating conditions. In this simulation model, both the output from the solar PV system and the wind generation system are connected to a common 105 V DC bus, which serves as the input voltage source for the proposed PBC. The controller block within the simulation model implements the SVCC arrangement for the parallel-connected DC-DC boost converters.

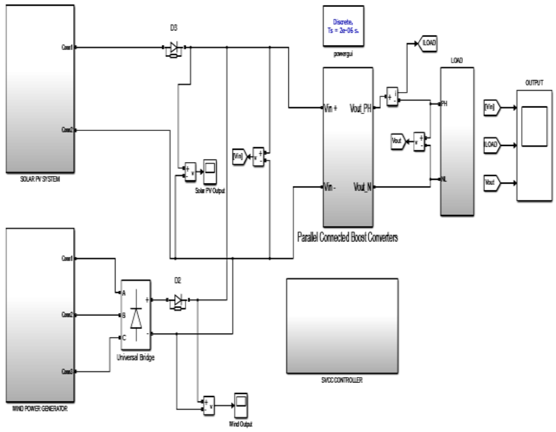


Figure 6. Simulink model of proposed PBC

This control scheme is essential for regulating the output voltage of the converters, ensuring stable and efficient operation across varying load conditions and input voltages. Additionally, the simulation model includes a load block that accommodates various power-rated loads. This component allows for testing the performance of the PBC under different load scenarios, evaluating how well the converter system adapts to changes in load demand while maintaining desired voltage levels and efficiency.

## 5. Simulation Results and Validation

In this section, several simulation output waveforms of the proposed system are presented.

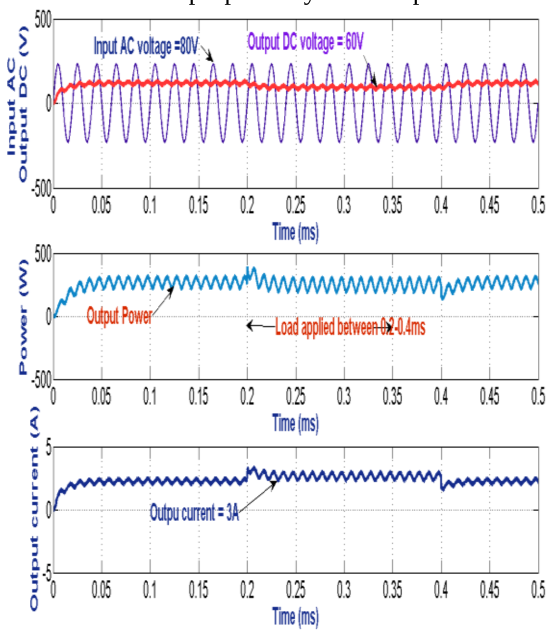


Figure 7. Input and output waveforms of the rectifier

Figure 7 illustrates the input and output waveforms of the rectifier, which is employed to convert the AC output voltage from the wind generator into DC voltage. The waveforms depicted include the input AC voltage, output DC voltage, output power, and output current of the rectifier. During the simulation period from 0.2 milliseconds to 0.4 milliseconds, a load is applied. It is noted that while there are no variations in the load voltage, both the output power and output current exhibit changes over time. This variation in power and current reflects the dynamic nature of the system's operation under varying load conditions, demonstrating how the rectifier converts the fluctuating AC voltage from the wind generator into a stable DC output for further use in the hybrid renewable energy system.

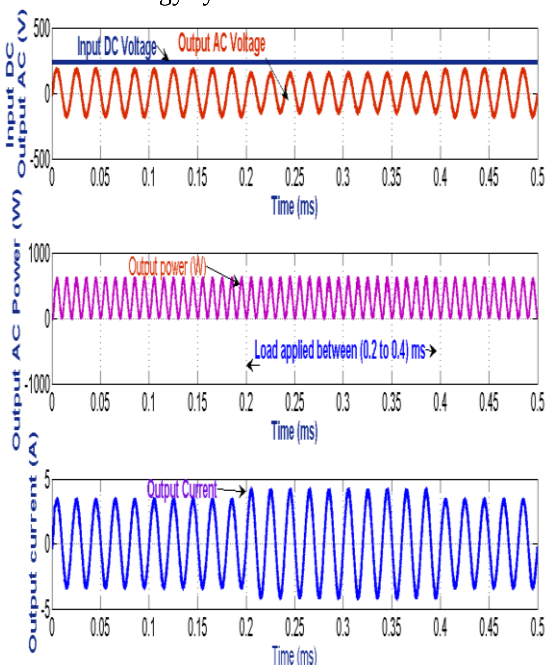


Figure 8. Input and output waveforms of PBC

In Figure 8, the input and output waveforms of the proposed parallel-connected boost converters are depicted. These waveforms include the input DC voltage, output AC voltage, output power, and output current of the converters. Throughout the time interval from 0.2 milliseconds to 0.4 milliseconds, the load applied to the converters is varied. Despite these load variations, the output voltage is effectively maintained at a constant value due to the operation of the proposed SVCC-based controller. This controller ensures stable and consistent output voltage from the converters, showcasing its capability to regulate and adapt to changes in load conditions during operation within the hybrid renewable energy system.

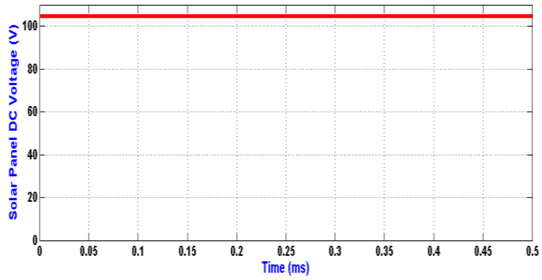


Figure 9. Solar panel output DC voltage

Figure 9 illustrates the DC voltage output from the solar panel, which is consistently regulated at 105 volts using the CPOT controller system. Similarly, Figure 10 shows the DC voltage from the wind energy system, which is also maintained at 105 volts. The wind system's DC voltage remains stable even with changes in load. Both the solar and wind system voltages are combined through a common DC bus, as shown in Figure 11, ensuring a constant voltage of 105 volts. This stable voltage enables smooth integration of both energy sources, promoting consistent operation.

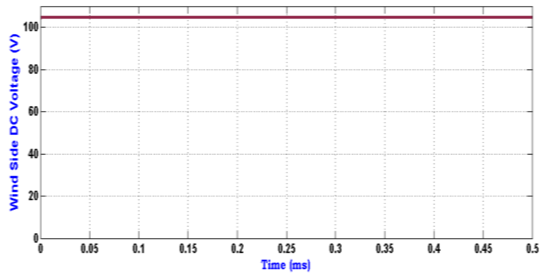


Figure 10. Wind side DC voltage

Solar and wind energy outputs typically fluctuate due to varying solar radiation and wind conditions. However, the CPOT controller, in conjunction with the P&O algorithm, efficiently regulates these fluctuations, ensuring a stable voltage output. Despite changes in environmental factors or load conditions, the proposed system consistently maintains reliable power delivery, enhancing the overall performance and stability of the hybrid energy system.

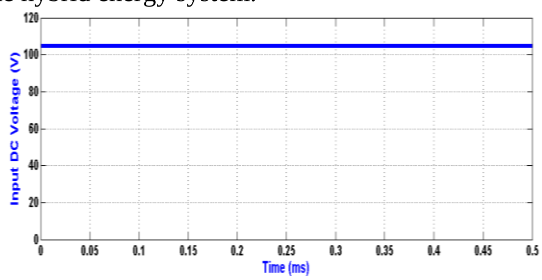


Figure 11. Common DC bus voltage of PBC

The proposed DC-AC converter is tested at varied loads of 40 and 100 watts, as shown in

Figure 12. According to Figure 12, the load currents are depicted varying in response to load fluctuations. Initially set at 60 watts from 0 to 0.2 milliseconds, the load increases abruptly to 100 watts and subsequently decreases to 40 watts by 0.4 milliseconds. These variations demonstrate the dynamic response of the system to changes in load demand. Figure 13 illustrates the output voltage of the parallel-connected boost converters, which is maintained at a constant 230 $V_{RMS}$ with a fundamental frequency of 50 Hz throughout the simulation period.

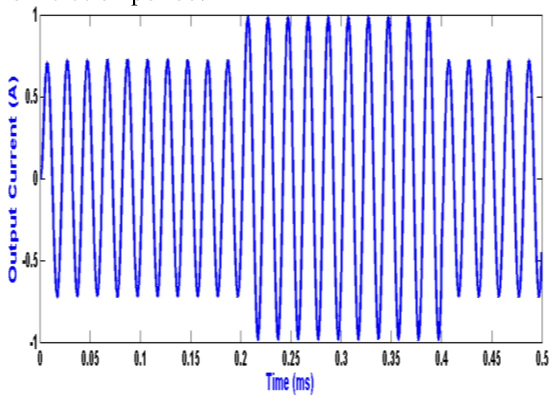


Figure 12. Output current of the PBC

This stable output voltage indicates effective regulation and control by the proposed system despite varying load conditions.

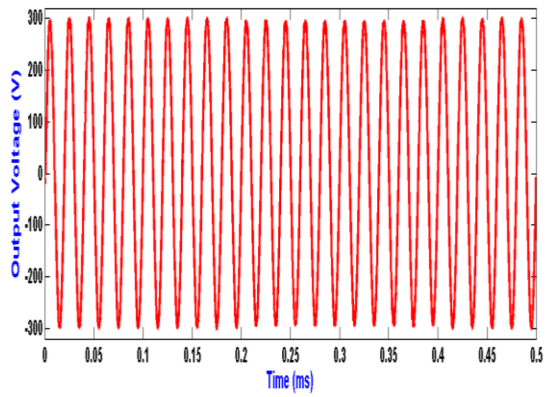


Figure 13. Output voltage of the PBC

Further analysis using fast fourier transform (FFT) for the output voltage of the parallel-connected boost converters was conducted over 25 cycles at the fundamental frequency of 50 Hz. FFT analysis reveals a THD of 2.19%, indicating that the proposed PBC has lower harmonic distortion compared to the multilevel inverter (MLI) [1], model predictive voltage controlled inverter (MPVI) [18], SPWM inverter (SPWMI) [19], and nine-level inverter (NLI) [21], as shown in the comparative analysis in Figure 14. The comparative analysis confirms the efficacy of the proposed design, revealing a lower THD value of 2.19%, thereby highlighting its practical effectiveness. Lower harmonic distortion values are desirable as they signify cleaner power output and reduced potential interference with electrical systems.

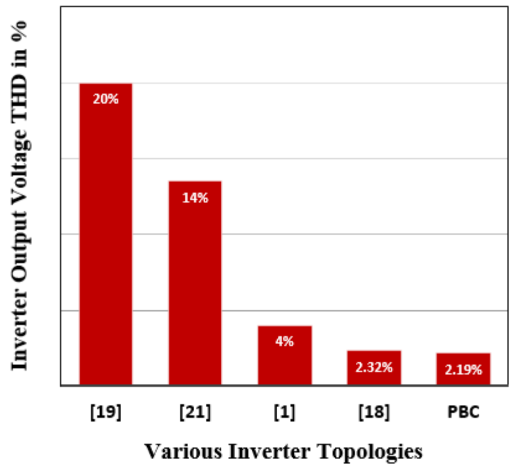


Figure 14. Comparative analysis of THD values in single-phase inverters

Table 2 compares the number of power conversion stages, the number of main switches used, and the THD values of various inverter topologies with the proposed PBC. From this comparison, the proposed PBC demonstrates single-stage power conversion, reduced losses due to fewer main switches, and lower distortion.

Table 2. Comparison of proposed PBC with Existing systems

| **Inverter Topology** | **Power Conversion Stages** | **Main Switches** | **THD (%)** |
|---|---|---|---|
| MLI [1] | 1 | 12 | 3.99 |
| MPVI [18] | 2 | 4 | 2.32 |
| SPWMI [19] | 1 | 4 | 20.00 |
| NLI [21] | 2 | 9 | 13.50 |
| Proposed PBC | 1 | 4 | 2.19 |

Overall, these simulation results validate the effectiveness of the proposed parallel-connected boost converters in maintaining stable output voltage and achieving low harmonic distortion under varying load conditions, thereby enhancing the performance and reliability of the hybrid renewable energy system. The proposed PBC integrates advanced SVCC methodology to optimize energy flow. These innovations collectively drive advancements in renewable energy, bolstered by simulation-based validation showcasing improved reliability and performance across diverse operational scenarios.

## 6. Conclusion

In this research, the sliding variable configuration control for parallel-connected boost converters marks a significant advancement in power conversion technology. A model for DC to AC conversion using a P&O algorithm-based CPOT controller for solar and wind renewable energy sources has been developed in the MATLAB/Simulink environment. This approach excels in voltage boosting during single-stage operation while maintaining a clean output voltage waveform without requiring additional filtering. The control method optimizes the use of solar PV and wind energy, demonstrating exceptional dynamic flexibility by promptly adjusting to fluctuating load conditions and input voltages in real-time. Unlike conventional fixed-parameter controls, the sliding variable approach allows for instant parameter adjustments, resulting in minimized overshoot, reduced steady-state errors, and significantly improved response times. These features collectively enhance voltage regulation, increase resilience against component variations and external disturbances, and boost overall efficiency by reducing THD in energy conversion systems. Future advancements will focus on exploring artificial neural networks to enhance the performance and stability of hybrid renewable energy systems. Additionally, thorough analyses of integration challenges and grid interaction issues will be conducted to ensure the smooth integration of renewable energy sources into existing power systems. Ultimately, this research will significantly contribute to accelerating the transition to sustainable energy alternatives by fostering the development of more reliable and efficient renewable energy systems.

### Nomenclature

| | |
|---|---|
| $V_{dc}$ | Input DC voltage (V) |
| $V_o$ | Parallel connected boost converters output voltage (V) |
| $V_{pv}$ | PV panel DC voltage(V) |
| $V_{ref}$ | Reference voltage (V) |
| $V_d$ | Equivalent circuit diode voltage (V) |
| $V_{bc1}$ | Voltages across the capacitor1 (V) |
| $V_{bc2}$ | Voltages across the capacitor2 (V) |
| $I_{PV}$ | PV panel DC current (Amp) |
| $I_m$ | Maximum current (Amp) |
| $I_{ref}$ | Reference current (Amp) |
| $I_{bc1}$ | Current of converter A (Amp) |
| $I_{bc2}$ | Current of converter B (Amp) |
| $r_L$ | Equivalent Resistance of the Circuit (Ω) |
| $r_D$ | Equivalent Resistance of the diode (Ω) |
| $\Delta$ | Vector differential operator |
| $S$ | Control signal |
| $U$ | Various switching states |
| $D_p$ | Duty cycle |
| $\bar{x}$ | Vector of the state variable $i_{L1}$ |
| $\bar{\bar{x}}$ | Vector of the state variable $V_{c1}$ |
| $\mathcal{E}_1$ | Difference of current (Amp) |
| $\mathcal{E}_2$ | Difference of voltage V) |
| $S_1$ | Switch 1 |
| $S_2$ | Switch 2 |
| $S_3$ | Switch 3 |
| $S_4$ | Switch 4 |
| $C_1$ | Capacitor 1 |
| $C_2$ | Capacitor 2 |
| $L_1$ | Inductor 1 |
| $L_2$ | Inductor 2 |
| $D_1$ | Diode 1 |
| $D_2$ | Diode 2 |
| *Rms* | Root mean square |
| *Fs* | Switching Frequency (KHz) |
| $\mu H$ | Micro Henry |
| $\mu F$ | Microfarad |

## Acknowledgements

This work was supported by the Vignan's Foundation for Science, Technology & Research (VFSTR), Guntur, and Andhra Pradesh, India.

## References

**[1]** Mohammadi Sheikhlari, A., & Sarvi, M. (2022). A multilevel inverter structure based on the development of full-bridge cells with the minimum number of switches for renewable energy applications. *Journal of Solar Energy Research*, 7(1), 971-982. DOI: 10.22059/JSER.2022.329155.1215

[2] Soundarya, G., Sitharthan, R., Sundarabalan, C. K., Balasundar, C., Karthikaikannan, D., & Sharma, J. (2021). Design and modeling of hybrid DC/AC microgrid with manifold renewable energy sources. *IEEE Canadian Journal of Electrical and Computer Engineering*, 44(2), 130-135. DOI: 10.1109/ICJECE.2020.2989222

[3] Silva, S., Laranjeira, E., & Soares, I. (2021). Health benefits from renewable electricity sources: A review. *Energies*, 14(20), 6678. DOI: 10.3390/en14206678

[4] Kong, L. G., Chen, X. L., Gong, J. H., Fan, D. J., Wang, B. L., & Li, S. (2022). Optimization of the hybrid solar power plants comprising photovoltaic and concentrating solar power using the butterfly algorithm. *Energy Conversion and Management*, 257, 115310. DOI:10.1016/j.enconman.2022.115310

[5] Alatai, S., Salem, M., Ishak, D., Das, H. S., Alhuyi Nazari, M., Bughneda, A., & Kamarol, M. (2021). A review on state-of-the-art power converters: Bidirectional, resonant, multilevel converters and their derivatives. *Applied Sciences*, 11(21), 10172.
. DOI: 10.3390/app112110172

[6] Ezhilvannan, P., Krishnan, S., Hemanth Kumar, B., Janardhan, K., & Ramachandran, S. (2023). Analysis of the effectiveness of a two-stage three-phase grid-connected inverter for photovoltaic applications. *Journal of Solar Energy Research*, 8(2), 1471-1483. DOI: 10.22059/JSER.2023.357025.1285

[7] Xu, Q., Vafamand, N., Chen, L., Dragičević, T., Xie, L., & Blaabjerg, F. (2020). Review on advanced control technologies for bidirectional DC/DC converters in DC microgrids. *IEEE Journal of Emerging and Selected Topics in Power Electronics*, 9(2), 1205-1221. DOI: 10.1109/JESTPE.2020.2978064

[8] Henao-Bravo, E. E., Saavedra-Montes, A. J., Ramos-Paja, C. A., Bastidas-Rodriguez, J. D., & Gonzalez Montoya, D. (2020). Charging/discharging system based on zeta/sepic converter and a sliding mode controller for DC bus voltage regulation. *IET Power Electronics*, 13(8), 1514-1527. DOI: 10.1049/iet-pel.2019.0746

[9] Alhuwaishel, F. M., & Enjeti, P. (2024, February). An electrolytic capacitor less non-isolated microinverter with integrated battery storage system for residential applications. *In 2024 IEEE Applied Power Electronics Conference and Exposition (APEC) (pp. 1275-1279). IEEE*. DOI: 10.1109/APEC48139.2024.10509351

[10] Karthikeyan, N., & Jebaselvi, G. A. (2024). A bidirectional four-port DC–DC converter for grid connected and isolated loads of hybrid renewable energy system using hybrid approach. *Analog Integrated Circuits and Signal Processing*, 1-21. DOI: 10.1007/s10470-024-02251-6

[11] Li, H., Wu, W., Huang, M., Chung, H. S. H., Liserre, M., & Blaabjerg, F. (2020). Design of PWM-SMC controller using linearized model for grid-connected inverter with LCL filter. *IEEE Transactions on Power Electronics*, 35(12), 12773-12786. DOI: 10.1109/TPEL.2020.2990496

[12] Haifeng W., Liu, Q., Bai, Z., Xie, G., Zheng, J., & Su, B. (2020). Thermodynamics analysis of a novel steam/air biomass gasification combined cooling, heating and power system with solar energy. *Applied Thermal Engineering*, 164, 114494. DOI: 10.1016/j.applthermaleng.2019.114494

[13] Pires, V. F., Cordeiro, A., Roncero-Clemente, C., Rivera, S., & Dragičević, T. (2022). DC-DC converters for bipolar microgrid voltage balancing: A comprehensive review of architectures and topologies. *IEEE Journal of Emerging and Selected Topics in Power Electronics*. DOI: 10.1109/JESTPE.2022.3208689

[14] Wu, L., Liu, J., Vazquez, S., & Mazumder, S. K. (2021). Sliding mode control in power converters and drives: A review. *IEEE/CAA Journal of Automatica Sinica*, 9(3), 392-406. DOI: 10.1109/JAS.2021.1004380

[15] Bist, N., & Sircar, A. (2021). Hybrid solar geothermal setup by optimal retrofitting. *Case Studies in Thermal Engineering*, 28, 101529. DOI: 10.1016/j.csite.2021.101529

[16] Masmoudi, A., Abdelkafi, A., Krichen, L., & Saidi, A. S. (2022). An experimental approach for improving stability in DC bus voltage of a stand-alone photovoltaic generator. *Energy*, 257, 124797. DOI: 10.1016/j.energy.2022.124797

[17] Josia, H. R. (2023). Off-Grid solar PV system design and analysis in isolated island for sustainable energy access: a case study in Sukun Island, Indonesia. *Journal of Solar Energy Research*, 8(3), 1609-1621. DOI: 10.22059/JSER.2023.360373.1318

[18] Talbi, B., Krim, F., Laib, A., & Sahli, A. (2020). Model predictive voltage control of a single-phase inverter with output LC filter for stand-alone renewable energy systems. *Electrical Engineering*, 102, 1073-1082. DOI: 10.1007/s00202-020-00936-5

[19] Ahmad, N. S., Tsai, T. W., & Chen, Y. M. (2020). Single-phase grid-connected inverters with simplified SPWM control. *IEEE Open Journal of Power Electronics*, 1, 170-179. DOI: 10.1109/OJPEL.2020.2996427

[20] Elnozahy, A., Yousef, A. M., Abo-Elyousr, F. K., Mohamed, M., & Abdelwahab, S. A. M. (2021). Performance improvement of hybrid renewable energy sources connected to the grid using artificial neural network and sliding mode control. *Journal of Power Electronics,* 21, 1166-1179. DOI: 10.1007/s43236-021-00242-8

[21] Arun, V., Sundaramoorthy, P., Nageswara Prasad, T., & Kumar, A. (2023). Asymmetrical single phase reduced switch nine level inverter with trinary sequence DC Input for PV based renewable energy systems. *Journal of Solar Energy Research,* 8(3), 1599-1608. DOI: 10.22059/JSER.2023.359014.1298

[22] Callegaro, L., Rojas, C. A., Ciobotaru, M., & Fletcher, J. E. (2021). A controller improving photovoltaic voltage regulation in the single-stage single-phase inverter. *IEEE Transactions on Power Electronics,* 37(1), 354-363. DOI: 10.1109/TPEL.2021.3100530

[23] Sreenivasulu Reddy, D., & Janamala, V. (2023). Optimal allocation of renewable sources with battery and capacitors in radial feeders for reliable power supply using pathfinder algorithm. *Journal of Solar Energy Research*, 8(4), 1651-1662. DOI: 10.22059/JSER.2023.358718.1299

[24] Hashemian, N., & Noorpoor, A. (2019). Assessment and multi-criteria optimization of a solar and biomass-based multi-generation system: Thermodynamic, exergoeconomic and exergoenvironmental aspects. *Energy Conversion and Management*, *195*, 788-797. DOI:10.1016/j.enconman.2019.05.039

[25] Darwish, A., Alotaibi, S., & Elgenedy, M. A. (2020). Current-source single-phase module integrated inverters for PV grid-connected applications. *IEEE Access*, 8, 53082-53096. DOI: 10.1109/ACCESS.2020.2981552

[26] Haq, I. U., Khan, Q., Ullah, S., Khan, S. A., Akmeliawati, R., Khan, M. A., & Iqbal, J. (2022). Neural network-based adaptive global sliding mode MPPT controller design for stand-alone photovoltaic systems. *Plos One,* 17(1), e0260480. DOI: 10.1371/journal.pone.0260480

[27] Ibrahim, A. W., Zhijian, F., Farh, H. M. H., Dagal, I., Al-Shamma'a, A. A., & Al-Shaalan, A. M. (2024). Hybrid SSA-PSO based intelligent direct sliding-mode control for extracting maximum photovoltaic output power and regulating the DC-bus voltage. *International journal of hydrogen energy,* 51, 348-370. DOI: 10.1016/j.ijhydene.2023.10.034

[28] Chigane, K., & Ouassaid, M. (2024). Experimental power control of a single-phase DC/AC converter using fuzzy integral sliding mode approach for photovoltaic systems. *International Journal of Dynamics and Control*, 12(2), 494-513. DOI: 10.1007/s40435-023-01198-2

[29] Tan, M. K., Moloney, B. O., Lim, K. G., Yang, S. S., Goh, H. H., & Teo, K. T. K. (2023). Fuzzy logic based perturb-and-observe algorithm for minimizing output fluctuation of a PV system. *In 2023 IEEE International Conference on Artificial Intelligence in Engineering and Technology (IICAIET) (pp. 319-324). IEEE*. DOI: 10.1109/IICAIET59451.2023.10291451

[30] Mousa, H. H., Youssef, A. R., & Mohamed, E. E. (2021). State of the art perturb and observe MPPT algorithms based wind energy conversion systems: A technology review. *International Journal of Electrical Power & Energy Systems,* 126, 106598. DOI: 10.1016/j.ijepes.2020.106598

[31] Trinh, H. A., Nguyen, D. G., Phan, V. D., Duong, T. Q., Truong, H. V. A., Choi, S. J., & Ahn, K. K. (2023). Robust adaptive control strategy for a bidirectional DC-DC converter based on extremum seeking and sliding mode control. *Sensors,* 23(1), 457. DOI: 10.3390/s23010457

[32] Khamharnphol, R., Kamdar, I., Waewsak, J., Chaichan, W., Khunpetch, S., Chiwamongkhonkarn, S., & Gagnon, Y. (2023). Microgrid hybrid solar/wind/diesel and battery energy storage power generation system: application to Koh Samui, Southern Thailand. *International Journal of Renewable Energy Development,* 12(2). DOI: 10.14710/ijred.2023.47761

[33] Farooqi, M. Z., Singh, B., & Panighiri, B. K. (2023). Performance enhancement of single-phase two-stage AC-DC converter with reduced DC-link capacitance. *IEEE Transactions on Industry Applications,* 59(5), 5739-5748. DOI: 10.1109/TIA.2023.3286381